Geochemistry Geophysics Geosystems G3

Article
Volume 13, Number 12
22 December 2012
Q12008, doi:10.1029/2012GC004417
ISSN: 1525-2027

Published by AGU and the Geochemical Society

Mantle flow in regions of complex tectonics: Insights from Indonesia

J. F. Di Leo and J. Wookey
School of Earth Sciences, University of Bristol, Bristol BS8 2UU, UK (jd7479@bristol.ac.uk)

J. O. S. Hammond
Department of Earth Science and Engineering, Imperial College London, London SW7 2AZ, UK

J.-M. Kendall
School of Earth Sciences, University of Bristol, Bristol BS8 2UU, UK

S. Kaneshima
Department of Earth and Planetary Sciences, Kyushu University, Fukuoka, Fukuoka 812-8581, Japan

H. Inoue and T. Yamashina
National Research Institute for Earth Science and Disaster Prevention, Tsukuba, Ibaraki 305-0006, Japan

P. Harjadi
Badan Meteorologi, Klimatologi dan Geofisika, Jakarta, Indonesia

[1] Indonesia is arguably one of the tectonically most complex regions on Earth today due to its location at the junction of several major tectonic plates and its long history of collision and accretion. It is thus an ideal location to study the interaction between subducting plates and mantle convection. Seismic anisotropy can serve as a diagnostic tool for identifying various subsurface deformational processes, such as mantle flow, for example. Here, we present novel shear wave splitting results across the Indonesian region. Using three different shear phases (local *S*, *SKS*, and downgoing *S*) to improve spatial resolution of anisotropic fabrics allows us to distinguish several deformational features. For example, the block rotation history of Borneo is reflected in coast-parallel fast directions, which we attribute to fossil anisotropy. Furthermore, we are able to unravel the mantle flow pattern in the Sulawesi and Banda region: We detect toroidal flow around the Celebes Sea slab, oblique corner flow in the Banda wedge, and sub-slab mantle flow around the arcuate Banda slab. We present evidence for deep, sub-520 km anisotropy at the Java subduction zone. In the Sumatran backarc, we measure trench-perpendicular fast orientations, which we assume to be due to mantle flow beneath the overriding Eurasian plate. These observations will allow to test ideas of, for example, slab–mantle coupling in subduction regions.

Components: 11,600 words, 10 figures.

Keywords: Indonesia; mantle flow; seismic anisotropy; shear wave splitting; subduction.

Index Terms: 7208 Seismology: Mantle (1212, 1213, 8124); 7240 Seismology: Subduction zones (1207, 1219, 1240); 8120 Tectonophysics: Dynamics of lithosphere and mantle: general (1213).

Received 29 August 2012; **Revised** 31 October 2012; **Accepted** 5 November 2012; **Published** 22 December 2012.

Di Leo, J. F., J. Wookey, J. O. S. Hammond, J.-M. Kendall, S. Kaneshima, H. Inoue, T. Yamashina, and P. Harjadi (2012), Mantle flow in regions of complex tectonics: Insights from Indonesia, *Geochem. Geophys. Geosyst.*, *13*, Q12008, doi:10.1029/2012GC004417.

1. Introduction

[2] Located at the quadruple junction of four major tectonic plates, namely the Indo-Australian, Eurasian, Philippine Sea, and Pacific plates, the Indonesian region is shaped by subduction, collision and accretion. It can hence be viewed as a tectonic setting analogous to primitive accretionary orogens [e.g., *Silver and Smith*, 1983; *Snyder and Barber*, 1997; *Hall*, 2009]. Several studies have been undertaken in the past few decades to shed light on this Rubik's cube of terranes and microplates; these include studies of surface geology [e.g., *Bader and Pubellier*, 2000], paleomagnetics [e.g., *Fuller et al.*, 1999], active source seismic reflection and refraction experiments [e.g., *Kopp et al.*, 1999], and GPS measurements [e.g., *Walpersdorf et al.*, 1998]. Although this provides us with a general understanding of the tectonic evolution of this complex region, a coherent picture of the subsurface processes, especially mantle flow through the maze of subducting slabs in eastern Indonesia, is still lacking.

1.1. Seismic Anisotropy and Shear Wave Splitting

[3] One approach to understanding deformational processes associated with a tectonic area is studying seismic anisotropy, the directional dependence of seismic wave speed. Seismic anisotropy is currently our best tool for determining *in situ* mantle flow direction. In the upper mantle, olivine crystals will align preferentially with finite strain (referred to as lattice-preferred orientation; LPO). The alignment is such that under dry mantle conditions, the olivine *a*-axis is parallel to the direction of mantle flow and the *b*-axis is perpendicular to the shear plane (A-type LPO [e.g., *Ribe*, 1989; *Babuška and Cara*, 1991; *Mainprice*, 2007]). The crust and the lithosphere, however, can also harbor numerous sources of anisotropy, both as LPO and SPO (shape-preferred orientation); these could be aligned cracks, potentially fluid- or melt-filled, oriented melt-pockets, or thin layers of materials with varying elastic properties [e.g., *Crampin and Booth*, 1985; *Kaneshima et al.*, 1988; *Kaneshima and Ando*, 1989; *Kendall et al.*, 2005; *Holtzman and Kendall*, 2010; *Bastow et al.*, 2010].

[4] A direct diagnostic of seismic anisotropy is shear wave splitting: upon encountering an anisotropic medium, a shear wave splits into two orthogonally polarized shear waves traveling at different velocities. Shear wave splitting is described by two parameters: the polarization of the faster shear wave (ϕ) and the delay time between the two waves (δt), which can both be measured, as outlined below. These two parameters can provide information about deformational processes as well as compositional properties. For example, in the case of A-type LPO of olivine in the upper mantle, the fast direction for a vertically propagating phase is parallel to the direction of mantle flow. Or, for SPO of cracks in the crust, the fast polarization parallels the alignment of fractures (provided their spacing is smaller than the seismic wavelength).

[5] The magnitude of δt is a function of both the strength of the anisotropy and the thickness of the anisotropic layer. The trade-off between these two parameters complicates placing spatial constraints on the anisotropy. Furthermore, shear wave splitting is a path-integrated, aggregate measurement, i.e., the exact location and extent of the anisotropy along the raypath cannot be determined from the measurement itself. The challenge, therefore, is to constrain the anisotropic fabrics both causally and spatially in light of the tectonic processes present. We approach this problem by using three different shear phases (local *S*, *SKS*, and downgoing *S*), as outlined in *Di Leo et al.* [2012]. Using different phases can improve vertical resolution beneath a receiver. In addition to that, source-side splitting can detect anisotropic fabrics where it is not possible to place seismic stations [e.g., *Nowacki et al.*, 2012].

[6] This is the first study of seismic anisotropy in the Banda and Flores Sea region and Borneo. We combine these novel results with observations of previous seismic anisotropy studies to gain a more coherent picture of the tectonic processes in the Indonesian region.

2. Tectonic Setting

[7] Indonesia consists of the Sundaland core and a patchwork of amalgamated terranes (Figure 1). Sundaland, the continental core of SE Asia [e.g.,

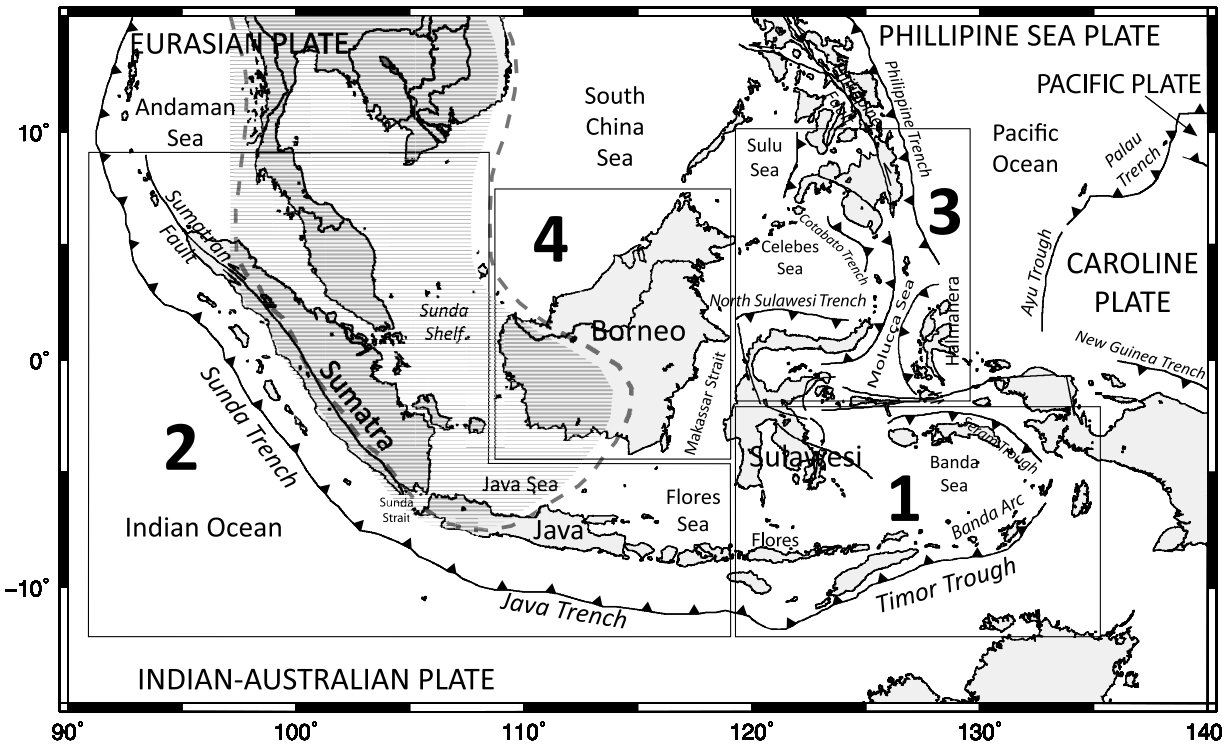

Figure 1. Map of Indonesia highlighting tectonic plate boundaries, subduction zones, and major faults. Subduction zones are denoted by barbed lines, with barbs indicating the direction of slab dip (redrawn after *Hall and Nichols* [1990]; *Hall* [1997]; *Macpherson et al.* [2003]; and *Djajadihardja et al.* [2004]). Hatched area marks the Sundaland continental core [after *Hall*, 2009]. Numbered boxes outline the regions discussed in this study: (1) southern Sulawesi and Banda Sea region; (2) Sumatra and Java; (3) northern Sulawesi, southern Philippines, and Molucca Sea region; and (4) Borneo.

Hamilton, 1979] is of Gondwanian origin and marks the present-day southeastern edge of the Eurasian plate. It encompasses the Thai–Malay Peninsula, Indochina, SW Borneo, Sumatra, Java, as well as the Sunda Shelf. The shelf was exposed during the Pleistocene and is still quite shallow today with water depths of around 200 m or less [e.g., *Hall*, 2009]. Due to the paucity of volcanic and seismic activity in the Sundaland core, several authors have described it as a craton or shield [e.g. *Ben-Avraham and Emery*, 1973; *Tjia*, 1996; *Barber et al.*, 2005]. However, unlike better established cratons or shields, such as the African craton or the Canadian shield, the Sundaland core is not underlain by cold thick lithosphere that has been consolidated since the Precambrian. Instead, the Sundaland core has undergone considerable internal deformation throughout the Meso- and Cenozoic, including the formation of several sedimentary basins and extensive faulting [*Hall and Morley*, 2004]. Furthermore, elevated surface heat flow of >80 mW/m^2 [*Artemieva and Mooney*, 2001] and low lithospheric and upper mantle velocities [e.g., *Widiyantoro and van der Hilst*, 1997; *Ritsema and van Heijst*, 2000] are indicative of a weak lithosphere, which, again, is uncharacteristic for a craton [*Hall and Morley*, 2004].

[8] Although we know that Indonesia is at the junction of several major tectonic plates, drawing exact plate boundaries remains challenging. *Gordon* [1998] labeled these 'diffuse plate' boundaries, noting they have, in fact, a width of between 200 and 1000 km, the exception being the Sunda trench, where the Indo-Australian plate is subducting beneath Eurasia. In eastern Indonesia, however, where there is a plethora of active and relict subduction zones, plate boundaries are more ambiguous.

[9] Since the mid-Mesozoic, several fragments that rifted from the Australian plate have successively attached themselves to the Sundaland margin. As a result, the SE Asian margin resembles an accretionary orogen in its early stages [*Hall*, 2009]. During the early Cretaceous, SW Borneo was added, followed by east Java, east Borneo, and western Sulawesi in the late Cretaceous. Further fragments, such as east Sulawesi, were added to the eastern margin in the Cenozoic [*Hall*, 2009].

[10] The oldest and most prominent subduction zone in the region is that of the Indo-Australian plate subducting beneath Eurasia at the Sunda trench with the Sunda arc having been active since the early Cenozoic [e.g., *Hamilton*, 1988; *Whittaker et al.*, 2007]. The exact timing of subduction initiation remains unknown; however, evidence suggests that it was not before 45 Ma [*Hall*, 2009]. Although this subduction zone appears to be continuous along Sumatra and Java, there is a sharp change in several characteristics at the Sunda strait, which separates Java from Sumatra. The age of the downgoing slab sharply increases from ∼60 Ma to ∼100 Ma between Sumatra and Java, respectively [*Sdrolias and Müller*, 2006]. Furthermore, the Sunda Strait marks a change in bulk sound speed within the slab [*Gorbatov and Kennett*, 2003], a decrease of deep seismicity below 500 km in Sumatra [e.g., *Engdahl et al.*, 1998], as well as a change in the distance between the volcanic front and the top of the slab from ∼90 km in Sumatra to ∼150 km in Java [*Syracuse and Abers*, 2006]. All these changes occur without being evident in the shape of the slab [*Gudmundsson and Sambridge*, 1998; *Syracuse and Abers*, 2006].

[11] Similarly, the transition from the Sunda to Banda subduction is not apparent from seismicity-derived slab contours [*Gudmundsson and Sambridge*, 1998; *Syracuse and Abers*, 2006]. However, the age of the volcanic arc increases markedly between eastern Java and the isle of Flores from ∼45 Ma [*Smyth et al.*, 2008] to <16 Ma [*Abbott and Chamalaun*, 1981; *Macpherson and Hall*, 2002], indicating different subduction histories for the two adjoining zones [e.g., *Hall*, 2012]. While oceanic lithosphere is being subducted at the Sunda trench, continental lithosphere is subducting at the Banda trench.

[12] The extremely curved Banda arc extends from Buru (south of Halmahera) over Seram and Timor to Flores (south of Sulawesi). It features an inner active volcanic arc and an outer non-volcanic arc. There has been a debate about whether the strong curvature is due to subduction of two slabs dipping toward each other [e.g., *Cardwell and Isacks*, 1978; *McCaffrey*, 1989] or bending of a single slab [e.g., *Hamilton*, 1979; *Hall*, 2002]. *Spakman and Hall* [2010] favor the view that the Banda arc formed during the mid-Miocene (∼15 Ma ago) by subduction of a Jurassic ocean embayment [e.g., *Hamilton*, 1979; *Charlton*, 2000; *Hall*, 2002] and that the shape is a result from the pre-existing bend in the impinging Australian plate margin as well as rollback of the Jurassic, hence old and cold, slab back to the curved shape of the embayment.

[13] The Sulawesi region northwest of the Banda arc exhibits the highest density of subduction zones in Indonesia. A unique feature of the area is double-sided subduction of the Molucca Sea plate in northern Sulawesi. This microplate is subducting westward at the Sangihe trench and eastward at the Halmahera trench. The two respective volcanic arcs are in the processes of colliding. This is the only arc–arc collision we can observe today [*Jaffe et al.*, 2004]. The northern part of the Molucca sea slab is flanked by two additional subduction zones dipping toward each other: the Philippine Sea plate is subducting westward beneath Mindanao peninsula [e.g., *Aurelio*, 1992], and the Celebes Sea plate, itself part of the Eurasian plate [*Hall and Nichols*, 1990], is subducting eastward beneath Mindanao [e.g., *Sajona et al.*, 1997]. Furthermore, the southern end of the Celebes Sea plate is subducting southwards beneath northern Sulawesi. Evidence suggests that the Celebes Sea slab and the Molucca Sea slab are colliding at a depth of ∼200 km [*Walpersdorf et al.*, 1998; *Kopp et al.*, 1999].

[14] West of Sulawesi lies the isle of Borneo, the perhaps most tectonically stable region in the study area today, as there is currently no active subduction around the island and, hence, little seismicity compared to the rest of Indonesia. The mid-Eocene (∼45 Ma ago), however, saw the onset of subduction of the Proto-South China Sea in the Sarawak Orogeny [*Hutchinson*, 2006]. Subduction lasted until the Early Miocene [e.g., *Hall et al.*, 2008]. Although Borneo has been a static part of the Sundaland core throughout the Cenozoic, palaeomagnetic data suggest that it has undergone a series of counter-clockwise rotations in the past as a consequence of convergence between the Eurasian and Indo-Australian plates: by ∼40° in the Early to mid-Cretaceous and again by ∼45–50° between 25 and 10 Ma ago [*Fuller et al.*, 1999].

[15] The Makassar Straits separating Borneo and Sulawesi formed during the Eocene through rifting [e.g., *Hamilton*, 1979; *Cloke et al.*, 1999]. The Wallace Line, i.e., the biogeographical boundary between the ecozones of Asia and Australasia, follows the Makassar Straits.

[16] This is, of course, only a brief outline of the tectonics of one of the geologically most complex regions on Earth today. For a more in-depth review, we refer the reader to *Lee and Lawrence* [1995], *Hall* [2002] or *Hall* [2012] and references therein,

for example. Nonetheless, it becomes clear that the region in its tectonic complexity and diversity cannot and should not be treated as one homogeneous landmass, especially when conducting a comprehensive study of seismic anisotropy, as we do here.

3. Previous Studies of Seismic Anisotropy in Indonesia

[17] The anisotropic structure of the Java–Sumatra subduction system was investigated by *Hammond et al.* [2010] using measurements of local *S* and *SKS* splitting (Region 2 in Figure 1). They observed anisotropy which they ascribed to trench-parallel aligned vertical cracks in the deforming overriding Eurasian plate as well as fossil anisotropy in the subducting slab. They noted several differences in slab characteristics beneath Sumatra and Java, such as location of the volcanic front [*Syracuse and Abers*, 2006], bulk sound speed [*Gorbatov and Kennett*, 2003], and slab age [*Sdrolias and Müller*, 2006], which they inferred to be the cause of differing splitting patterns for Java and Sumatra.

[18] In a recent study [*Di Leo et al.*, 2012], we investigated the anisotropic characteristics of the Sangihe subduction zone, which extends from the southern Philippines to northern Sulawesi (Region 3 in Figure 1). As in this study, we used three different shear phases in the splitting analysis, and were thus able to distinguish three regions of anisotropy at this subduction zone: one in the overriding Eurasian plate due to fossil anisotropy as well as SPO of melt-filled cracks, one atop the subducting slab due to shear layers with very strong olivine LPO in the deep mantle wedge, and one beneath the slab due to trench-parallel sub-slab mantle flow beneath the Molucca Sea microplate.

[19] In this study, we present new shear wave splitting measurements for parts of Indonesia - such as the Banda Sea region, southern Sulawesi, and Borneo (Regions 1 and 4 in Figure 1) - previously unstudied with seismic anisotropy. However, we also revisit aspects of the studies mentioned above and add new shear wave splitting results in the backarc regions of Java and Sumatra.

4. Data and Methodology

[20] We analyze three different shear phases, local *S*, *SKS*, and teleseismically recorded *S* waves, to attain an improved spatial resolution of anisotropic fabrics in the Indonesian subduction system and Borneo.

[21] The majority of the data used for local *S* and *SKS* splitting analysis comes from the temporary JISNET (Japan Indonesia Seismic Network) array [*Ohtaki et al.*, 2000], which recorded from 1998 to 2007, with some stations having been reactivated recently. Recordings from some stations of this network were examined in the previous studies of *Hammond et al.* [2010] and *Di Leo et al.* [2012]. In this study, we use 5 years of data (1998–2003) recorded by JISNET stations TOLI, PCI, and KDI on Sulawesi, TARA, BKB, PKBI, and PTK in Kalimantan (the Indonesian part of Borneo), TPI on Belitung Island, TPN on the Riau Islands. In addition to that, we use recordings from GSN (Global Seismographic Network) stations BTDF in Singapore (1998–2006) and KAPI on Sulawesi (1999–2010), as well as GEOFON station LUWI on Sulawesi (2008–2010) (Figures 2, 5, and 8 and Table S1 in the auxiliary material).[1]

[22] The data used in the source-side splitting analysis were recorded by five GEOSCOPE stations located in Russia (SEY), China (WUS), India (HYB), Australia (CAN), and Antarctica (DRV) and one K-NET station in Kyrgyzstan (AAK) (Figure 3 and Table S1 in the auxiliary material).

[23] Data were filtered using Butterworth bandpass filters with corners between 0.1 and 1 Hz in the case of source-side *S* and local *S* data, and 0.03 and 0.4 Hz for *SKS* data. Overlapping filter bands for the different shear phases should decrease any influence of frequency dependent anisotropy. Nonetheless, we applied low frequency filters to local *S* data to test for frequency dependence, but could not detect any evidence for it.

[24] We measure shear wave splitting from three-component seismic data following the method of *Silver and Chan* [1991]. It grid-searches for the two splitting parameters, direction of the fast shear wave (ϕ) and delay time (δt), that minimize the second eigenvalue of the covariance matrix of the particle motion, thereby correcting for the splitting. The cluster analysis method of *Teanby et al.* [2004] allows removal of subjectivity regarding the choice of window lengths around the shear phases [*Wüstefeld et al.*, 2010]. Examples of shear wave splitting results are shown in Figure 4.

[25] For source-side splitting, we use events that originate in the study area and are recorded at teleseismic distances between 50° and 85° [*Wookey et al.*, 2005; *Di Leo et al.*, 2012]. The method relies on the assumption that the lower mantle

[1] Auxiliary materials are available in the HTML. doi:10.1029/2012GC004417.

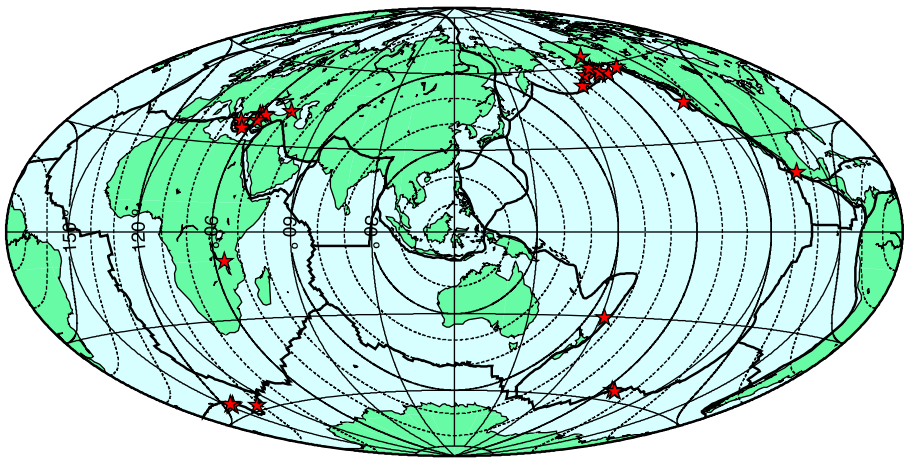

Figure 2. Teleseismic earthquakes (red) used in the *SKS* splitting analysis.

above *D″* is insignificantly anisotropic. A number of studies have suggested this to be the case [e.g., *Meade et al.*, 1995; *Montagner and Kennett*, 1996; *Panning and Romanowicz*, 2006; *Kustowski et al.*, 2008]. Therefore, we assume that the measured anisotropic fabrics are located in the upper 660 km beneath the receiver and the source. Provided the receiver-side anisotropy is well constrained (i.e., sufficient measurements with results showing little to no backazimuthal variation, thus indicating simple one-layer anisotropy [*Silver and Savage*, 1994]), it can be removed in the splitting analysis. The remaining splitting must therefore stem from the source-side. Splitting parameters for these upper mantle corrections were taken from *SKS* splitting studies by *Barruol and Hoffmann* [1999] and *Wolfe and Vernon* [1998].

[26] In order to make the source-side splitting results comparable with those of *SKS* and local *S*

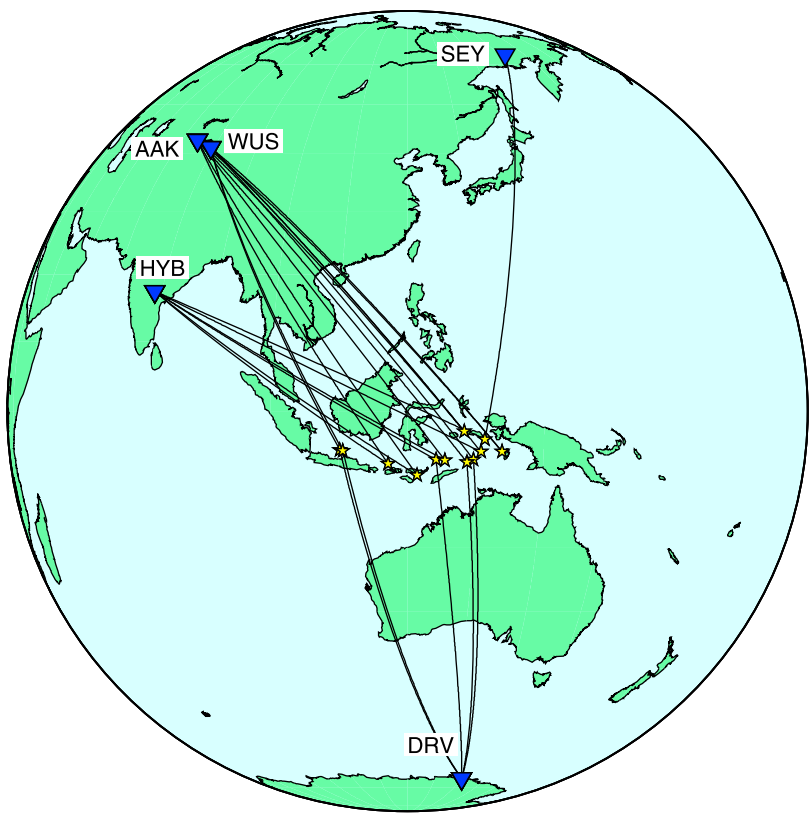

Figure 3. Earthquakes (yellow) used in the source-side splitting analysis.

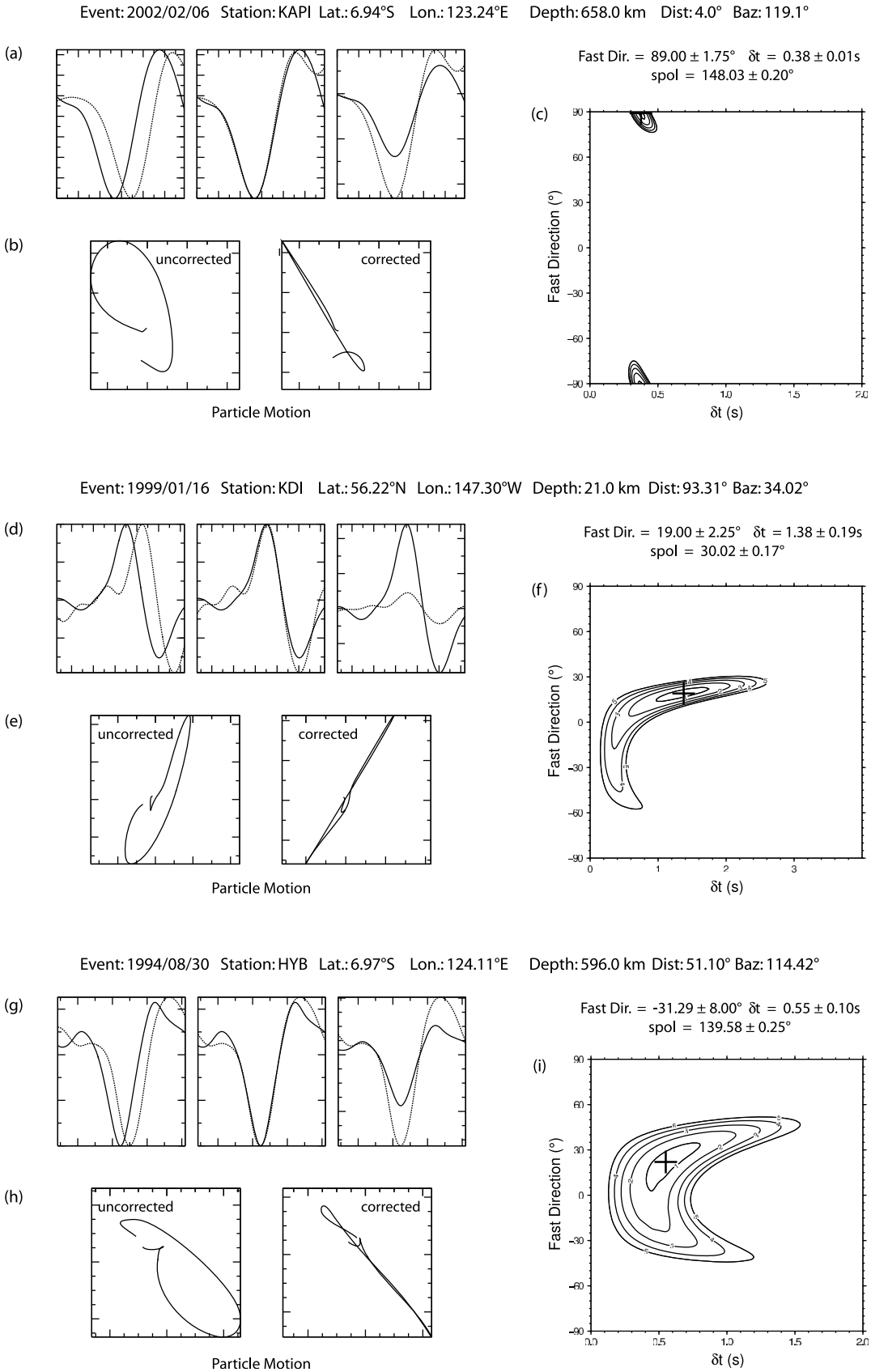
Event: 2002/02/06 Station: KAPI Lat.: 6.94°S Lon.: 123.24°E Depth: 658.0 km Dist: 4.0° Baz: 119.1°
(a)
(b)
uncorrected
corrected
Particle Motion
Fast Dir. = 89.00 ± 1.75° δt = 0.38 ± 0.01s
spol = 148.03 ± 0.20°
(c)
Fast Direction (°)
δt (s)
Event: 1999/01/16 Station: KDI Lat.: 56.22°N Lon.: 147.30°W Depth: 21.0 km Dist: 93.31° Baz: 34.02°
(d)
(e)
uncorrected
corrected
Particle Motion
Fast Dir. = 19.00 ± 2.25° δt = 1.38 ± 0.19s
spol = 30.02 ± 0.17°
(f)
Fast Direction (°)
δt (s)
Event: 1994/08/30 Station: HYB Lat.: 6.97°S Lon.: 124.11°E Depth: 596.0 km Dist: 51.10° Baz: 114.42°
(g)
(h)
uncorrected
corrected
Particle Motion
Fast Dir. = -31.29 ± 8.00° δt = 0.55 ± 0.10s
spol = 139.58 ± 0.25°
(i)
Fast Direction (°)
δt (s)

Figure 4

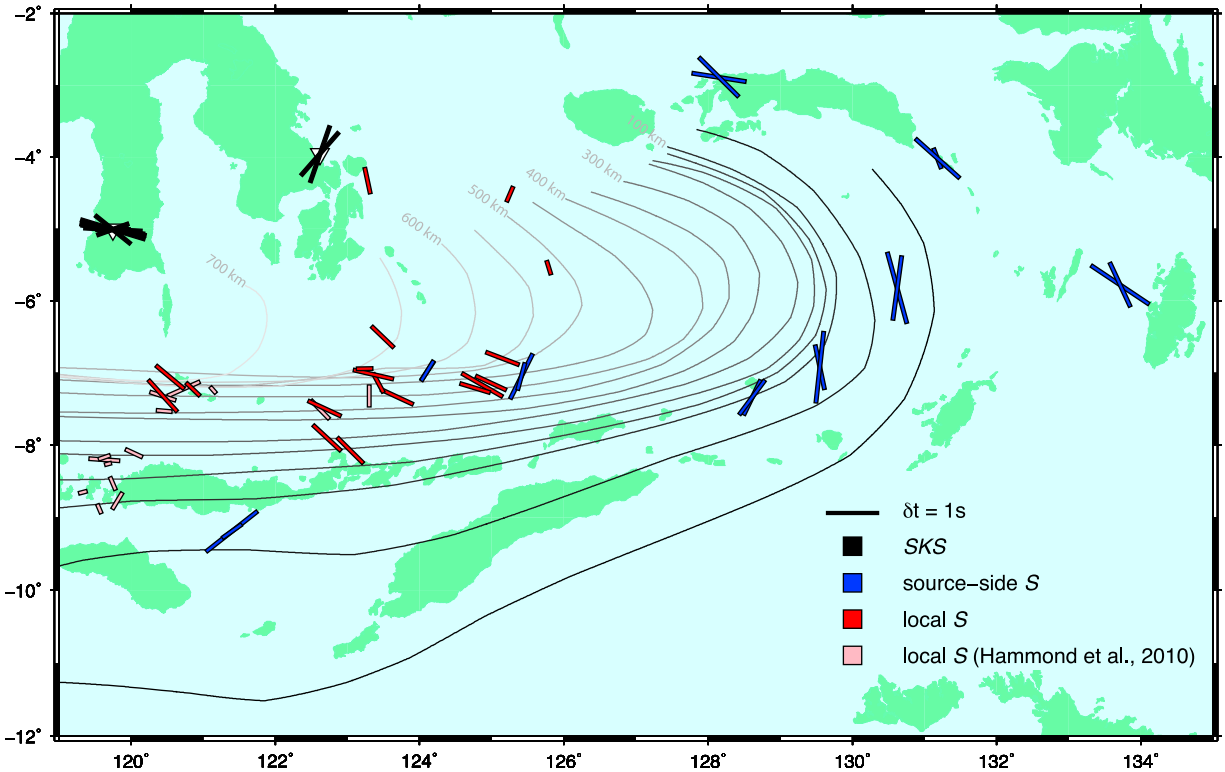

Figure 5. Region 1: Shear wave splitting results for the Banda Sea region. Bars are oriented in the fast direction and colored by phase type (black for *SKS*, blue for source-side *S*, pink for local *S* measurements by *Hammond et al.* [2010], red for local *S* of this study). Their length is proportional to δt. White inverted triangles are seismic stations. *SKS* results are plotted at the station, local and source-side *S* results are plotted at the source. Grey lines are slab contours in 50 km intervals [*Gudmundsson and Sambridge*, 1998].

measurements, one has to rotate the measured fast direction (after the receiver-side correction) from the geographical reference frame of the receiver to that of the source. This is done with $\phi'' = azimuth + backazimuth - \phi$, where ϕ'' is the source-side fast direction and ϕ is corrected receiver-side fast direction. Only events that have been recorded by two or more stations and yield consistent results are used (Figure 3 and Table S4 in the auxiliary material).

5. Results

[27] In the following, we discuss results separately for the different regions. Results are shown in Figures 5–6 and listed in Tables S2–S4 in the auxiliary material.

5.1. Region 1: Southern Sulawesi and the Banda Sea

[28] We analyzed recordings from two broadband stations in southern Sulawesi: KAPI in the southwest and KDI in the southeast. For KAPI, we obtained 8 good quality *SKS* splitting measurements with a stacked average of δt = 1.13 s (calculated using the stacking technique of *Wolfe and Silver* [1998]) (Figure 5). Fast directions are consistently E–W trending, parallel to the Sunda–Banda trench. Unfortunately, all 8 rays have similar backazimuths, thereby making it impossible to rule

Figure 4. Example of three shear wave splitting measurements using the method of *Silver and Chan* [1991] and *Teanby et al.* [2004]. (top) Local *S* splitting result for station KAPI. (middle) *SKS* splitting result for KDI. (bottom) Source-side *S*-wave splitting result for HYB. (a, d, g) Fast and slow waveforms, (left) uncorrected and (middle: normalized; right: real amplitudes) corrected. (b, e, h) Particle motion before and after correction. Good results show elliptical particle motion before and linear particle motion after correction. (c, f, i) A grid search determines the optimal fast direction and delay time (cross), which linearize the particle motion, thereby correcting for the splitting. Note the different timescales for δt. The first surrounding contour marks the 95% confidence region.

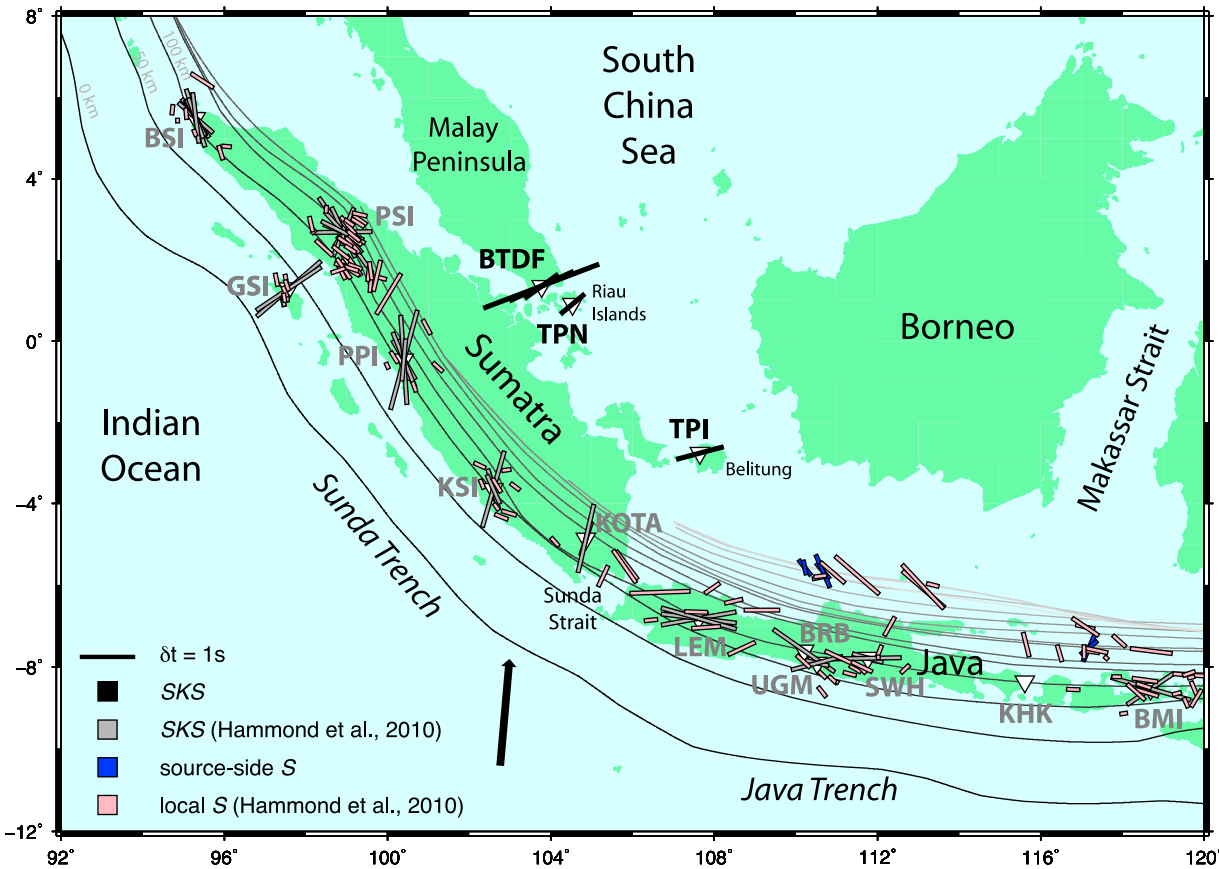

Figure 6. Region 2: Shear wave splitting results for the Sumatra–Java region. Bars are oriented in the fast direction and colored by phase type (gray for *SKS* results of *Hammond et al.* [2010], black for *SKS* measurements of this study, blue for source-side *S*, pink for local *S* measurements by *Hammond et al.* [2010]). Their length is proportional to δt. White inverted triangles are seismic stations. *SKS* results are plotted at the station, local and source-side *S* results are plotted at the source. Grey lines are slab contours in 50 km intervals [*Gudmundsson and Sambridge*, 1998]. Black arrow marks absolute plate motion (~75 mm/yr; NUVEL1A) [*Gripp and Gordon*, 1990].

out any backazimuthal variation in splitting to indicate whether there is one horizontal or dipping layer of anisotropy or several layers [*Silver and Savage*, 1994]. The two *SKS* measurements at KDI have δt of 1.32 and 1.38 s, and ϕ is NE–SW, approximately parallel to the curvature of the Banda Arc. These two rays have very similar backazimuths as well.

[29] We obtained 7 local *S* splitting measurements for KAPI and 11 for KDI. All 18 events are deep with depths of ~460–690 km. Time-lags measured at KAPI are 0.38–0.95 s and 0.34–1.08 s at KDI. Fast orientations are predominantly NW–SE trending, oblique to the subducting slab with a trend toward perpendicular.

[30] Source-side splitting analysis yielded 18 measurements for 9 events in the Banda Sea region. Five events are fairly shallow with depths between ~33 km and 54 km, two earthquakes are of intermediate depth (~97 and 143 km), and two originate within the mantle transition zone at depths 533 km and 596 km. Delay times vary between 0.50 s and 1.70 s. Apart from the two deep events, fast polarizations roughly follow the curvature of the Banda Arc.

5.1.1. Anisotropy in the Banda Sea Slab?

[31] In order to determine if there are measurable anisotropic fabrics in the subducting Banda Sea slab, we test whether there is a correlation between measured delay time and path length of each respective ray within the slab. We use the same approach as *Di Leo et al.* [2012]. We built a 3-D model of the slab based on the seismicity-derived Regional Upper Mantle (RUM) model by *Gudmundsson and Sambridge* [1998] and the iasp91 1-D velocity model [*Kennett and Engdahl*, 1991]. Although there are more recent slab models by *Syracuse and Abers* [2006] and *Hayes et al.* [2012], they do not image

the westernmost extent of the slab (i.e., the Banda arc), which is of great importance for the interpretation of our splitting measurements in that area. Our slab model has a thickness of 100 km, which is generally considered to be a typical value for most slabs [e.g., *Bercovici and Karato*, 2003]. Furthermore, this makes our results comparable to those of *Hammond et al.* [2010], who also used 100 km slab thickness in their modeling. Using the TauP Toolkit of *Crotwell et al.* [1999] and *Winchester and Crotwell* [1999], we raytrace through the model and compare the estimated path length of each ray within the slab to the measured delay time (Figure 9). We assume the 1-D raypaths to be approximate to the actual path. If the slab harbors significant seismic anisotropy, δt should increase with increasing slab path length. Local *S* rays traversing the slab show no increase in δt with slab path. For those downgoing *S* phases traveling through the slab, however, there appears to be an increase in time-lag. This indicates that the deep slab, i.e., that part of the slab not sampled by upgoing local *S* waves, may well be anisotropic.

5.2. Region 2: Sumatra and Java

[32] Recordings from stations in the backarc region of Sumatra (BTDF, TPN, TPI) yielded 5 *SKS* splitting measurements: 3 for BTDF and one each for TPN and TPI (Figure 6). Delay times are quite variable, ranging from 0.68 to 2.73 s. At BTDF alone, lag-times are between 0.90 and 2.73 s with a stacked average of ~1.10 s. At all three stations, fast directions are consistently NE–SW trending.

[33] Three deep events, with depths between ~535 and 636 km, in the backarc region of Java fulfilled our criteria and rendered source-side splitting results. Delay times are between 0.33 and 0.79 s. Fast polarizations are NW–SE trending for the two westernmost events and NE–SW trending for the event at the southern end of the Makassar Straits.

[34] No local *S* measurements were obtained for these three stations.

5.3. Region 3: Northern Sulawesi and the Molucca Sea

[35] We analyzed data from three stations in northern Sulawesi: TOLI, PCI, and LUWI. We obtained 10 good-quality *SKS* splitting measurements for these stations: 4 for TOLI, 4 for LUWI, and 2 for PCI (Figure 7). Lag-times show stacked averages 1.25 s, 1.30 s, and 0.98 s, respectively. Fast directions are roughly, but consistently, E–W trending. *SKS* phases recorded at PCI have similar backazimuths. At TOLI and LUWI, however, the rays have different backazimuths, but similar ϕ, which is indicative of a single, horizontal layer of anisotropy.

[36] We obtained 6 local *S* splitting results for the region: 4 for PCI and 2 for LUWI; none for TOLI, however. Fast directions measured at both stations are predominantly NNW–SSE trending. Delay times for the PCI results are between 0.36 and 0.54 s; for LUWI, 0.30 and 0.60 s.

5.4. Region 4: Borneo

[37] Data recorded at 4 stations in Kalimantan on Borneo, TARA, BKB, PKBI, and PTK, yielded 7 *SKS* splitting results (Figure 8). Due to the lack of seismicity in the region, no local *S* or source-side splitting was measured. Delay times vary between 0.55 s and 1.35 s. Fast directions tend to be parallel to the coast line. Backazimuths of the events used are all too similar to determine whether there is more than one horizontal layer of anisotropy present.

6. Discussion

[38] Our new measurements of shear wave splitting in Indonesia, in conjunction with previous studies, contribute to unraveling various tectonic processes in this complex area, highlighting the fact that the landmass conveniently labeled Indonesia ought not to be treated as one homogenous region, e.g., when conducting studies of global mantle flow.

6.1. Region 1: Southern Sulawesi and the Banda Sea

[39] We believe the anisotropy detected by both the *SKS* and local *S* splitting to be caused by mantle flow in the Banda wedge. Due to the strong curvature and obliquity of the Banda subduction zone, corner flow in the wedge is not as two-dimensional as in regular subduction zones (Figure 10). The interior of the wedge generally does not produce large amounts of anisotropy [e.g., *Buttles and Olson*, 1998; *Di Leo et al.*, 2012]. Thus, the two different phases may be sensitive to two different aspects of this same corner flow: The deep local events may be detecting shear layers at the bottom of the wedge, immediately above the slab. In that region, strain and shear stress are extremely high and progressive simple shear can thus produce very strong olivine LPO [*Ribe*, 1989]. Several studies have predicted these supra-slab shear layers numerically [*McKenzie*, 1979; *Ribe*, 1989;

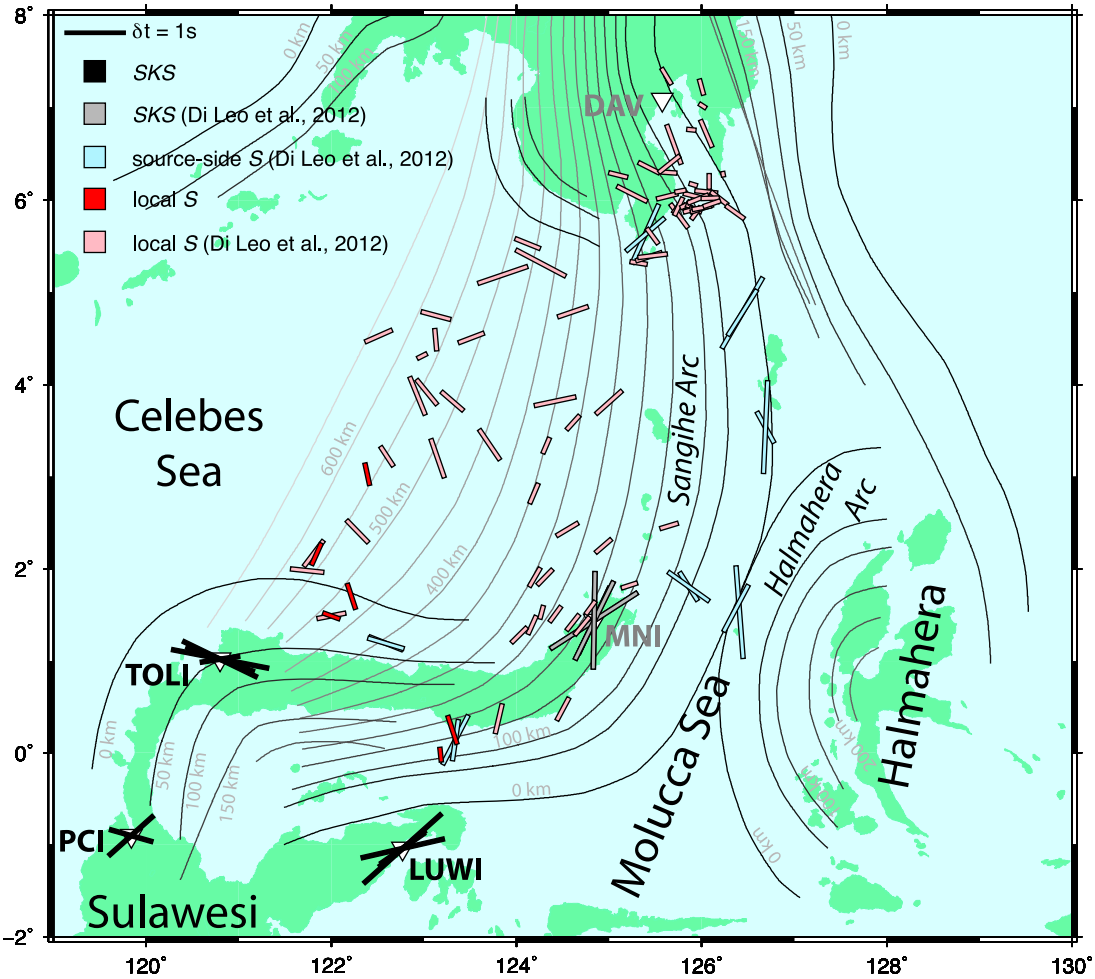

Figure 7. Region 3: Shear wave splitting results for the Molucca Sea region. Bars are oriented in the fast direction and colored by phase type (gray for *SKS*, light blue for source-side *S* and pink for local *S* results of *Di Leo et al.* [2012], respectively; red for local *S* and black for *SKS* measurements of this study). Their length is proportional to δt. White inverted triangles are seismic stations. *SKS* results are plotted at the station, local and source-side *S* results are plotted at the source. Grey lines are slab contours in 50 km intervals [*Gudmundsson and Sambridge*, 1998].

Kendall and Thomson, 1993], and they have been observed in analog models [*Buttles and Olson*, 1998] and seismically in the Sangihe subduction zone [*Di Leo et al.*, 2012]. In the latter study, delay times measured for these shear layers are similar to those measured at KAPI and KDI, making it possible that they are being caused by the same mechanism. This region of strong LPO at the slab–wedge interface is only fully developed below ~200 km depth and has a thickness of ~100 km [*Buttles and Olson*, 1998] or an angular width of ~5–10° [*Ribe*, 1989]. *SKS* rays recorded at KDI and KAPI do not traverse this part of the subduction zone. Corresponding time-lags are of similar magnitude as those arising from mantle flow at the Sangihe subduction zone in northern Sulawesi [*Di Leo et al.*, 2012]. Fast directions are approximately parallel to the curvature of the Banda arc. We therefore suggest that the anisotropy measured at the two stations in southern Sulawesi is due to mantle flow around the continental keel of the island, parallel to the arcuate Banda slab. The resulting picture is that of oblique corner flow - i.e., neither trench-parallel nor perpendicular - in the wedge of the Banda subduction zone.

[40] Source-side splitting fast directions of the four northeasternmost shallow events (~0–50 km) in Region 1 appear to parallel the curvature of the Banda arc (Figure 5). We suggest that this anisotropy may be caused by trench-parallel mantle flow below the Banda slab (Figure 10). Trench-parallel sub-slab mantle flow has been observed in several subduction zones, for example, in the Sangihe subduction zone [*Di Leo et al.*, 2012], the Caribbean [*Piñero-Feliciangeli and Kendall*, 2008] or New Zealand [*Gledhill and Gubbins*, 1995; *Greve*

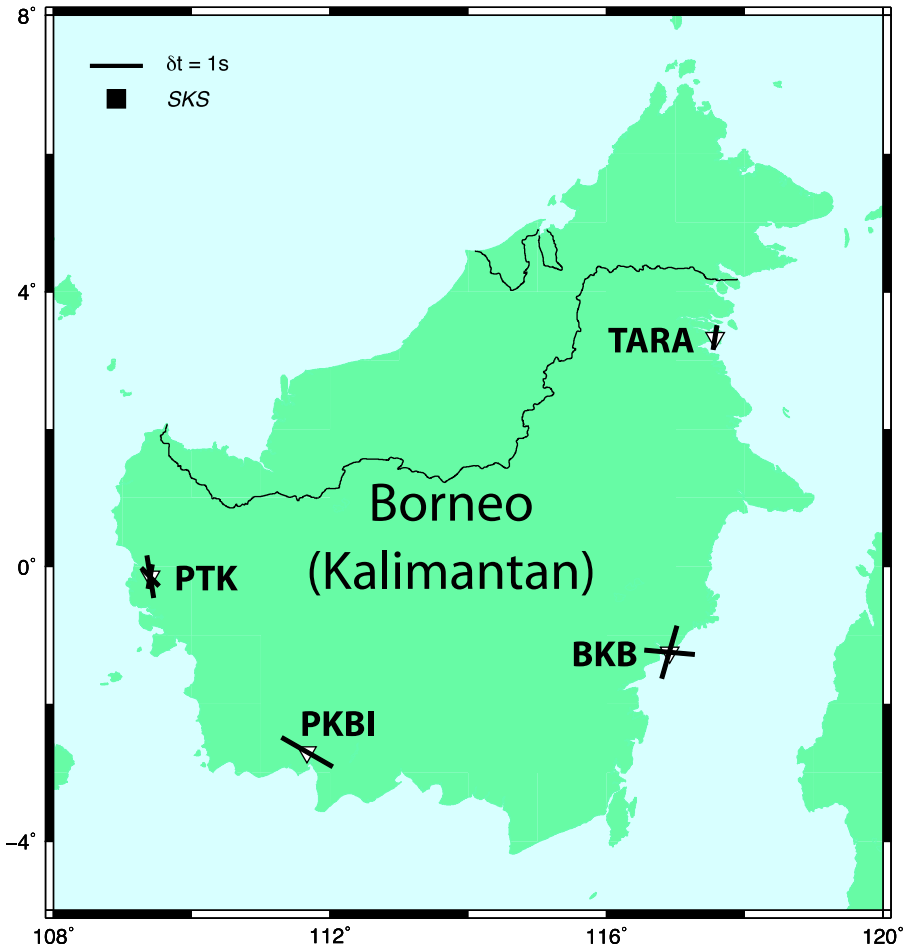

Figure 8. Region 4: *SKS* splitting results for Kalimantan, the Indonesian part of Borneo. Black bars are oriented in the fast direction, their length is proportional to δt. White inverted triangles are seismic stations.

et al., 2008] (for reviews, see *Long and Silver* [2009] and *Long and Becker* [2010]). One possible cause of trench-parallel mantle flow is slab rollback, which in the case of the Banda subduction zone is clearly observed [e.g., *Spakman and Hall*, 2010].

[41] Splitting measurements of the two deep events (>530 km; off the southeastern tip of Sulawesi) as well as the splitting results for the two earthquakes around 7.5°S and 129°E, on the other hand, are sensitive to deeper anisotropy, presumably deep within the slab (Figure 9). Since old, cold, Jurassic continental crust is being subducted at the Banda trench, it is possible that the slab - unlike younger, thinner slabs - has retained measurable fossil anisotropy. Alternatively, the two deep events may be detecting anisotropy in the mantle transition zone, as discussed below (see section 6.2.2). The fast directions of these two deep events are nearly perpendicular to those measured with local *S* phases in the same area, indicating that the two phases are detecting two different regions of anisotropy: above the slab and deep within or below. Irrespective of the source of this deep anisotropy, this locality is an excellent example of how using different shear phases can significantly improve spatial resolution of seismic anisotropy.

6.2. Region 2: Sumatra and Java

6.2.1. The Sunda–Banda Transition: Evidence From Fossil Anisotropy

[42] The transition from the Sunda to the Banda subduction zone, i.e. from subduction of oceanic to continental lithosphere, is not evident in seismicity-derived slab models [*Gudmundsson and Sambridge*, 1998; *Syracuse and Abers*, 2006; *Hayes et al.*, 2012]. *Hammond et al.* [2010] measured highly varied fast directions from local *S* splitting at JISNET station BMI (Figures 5 and 6), which is located atop this

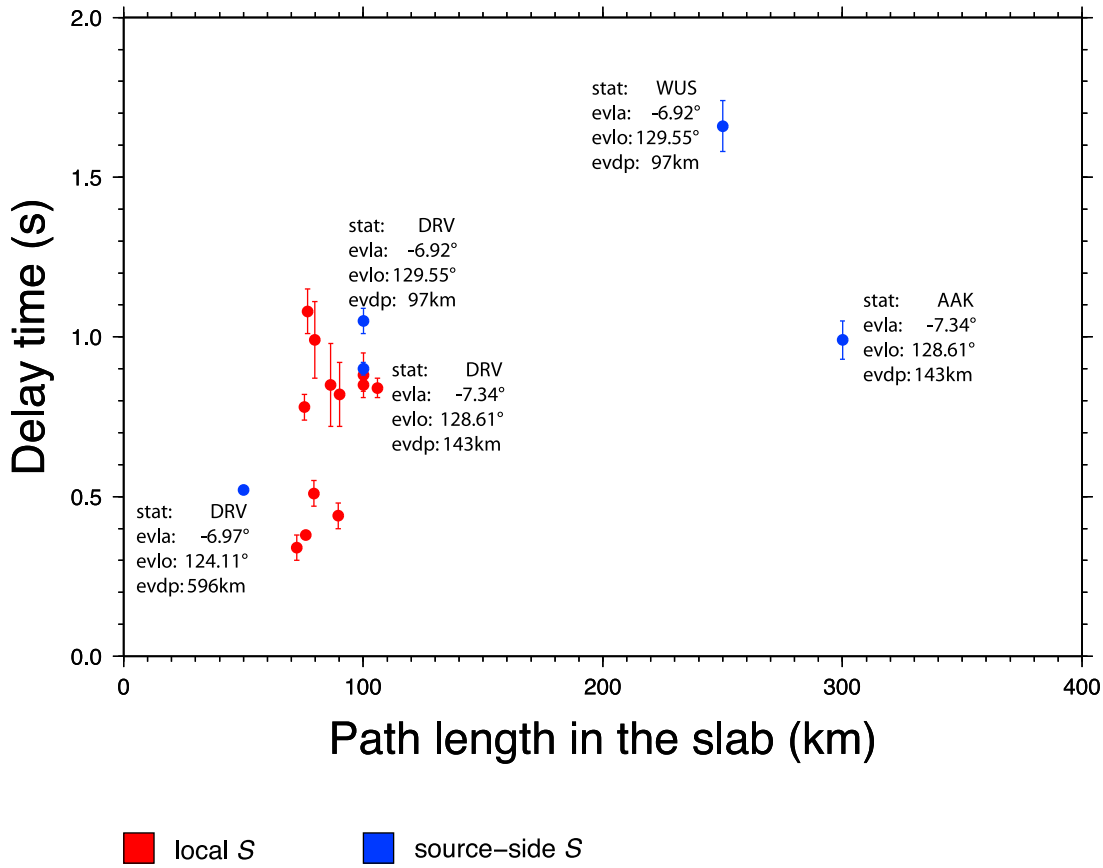

Figure 9. Delay time (δt) as a function of estimated path length of rays within the Banda Sea slab. Event information is given for the source-side *S* measurements (stat: station name; evla: event latitude; evlo: event longitude; evdp: event depth). Local *S* measurements (red) show no increase of δt with slab path length. Source-side *S* measurements (blue), however, do show an increase in time-lag with slab path length. This suggests that there may perhaps be seismic anisotropy in the deep slab interior that is not being detected by local *S* rays.

transition zone between the two subduction zones. Therefore, these contorted anisotropic fabrics may perhaps stem from fossil anisotropy frozen into this boundary zone between the two slab fragments. The joining of the two plate fragments is sure to have been accompanied by high stresses and strains, and the fossil anisotropy is the remaining evidence thereof.

6.2.2. Anisotropy in the Mantle Transition Zone

[43] Three deep-focus events (between 535 and 636 km depth) yield source-side *S* splitting results with delay times between ~0.33 s and 0.79 s, giving evidence to deep anisotropic fabrics within the transition zone (TZ). Three mineral phases dominate volumetrically in the TZ: wadsleyite, ringwoodite, and garnet. Of these, only wadsleyite has significant intrinsic elastic anisotropy [*Mainprice et al.*, 1990] and the potential to induce *S* wave anisotropy of ~1% [*Tommasi et al.*, 2004; *Demouchy et al.*, 2011]. Ringwoodite and garnet do not appear to produce significant anisotropy [e.g., *Carrez et al.*, 2006; *Tommasi and Mainprice*, 2008]. However, wadsleyite is only abundant in the upper TZ, i.e., above 520 km. With the source-side events being below ~535 km, another mechanism or mineral phase need to be invoked.

[44] A likely candidate is a dense hydrous magnesium silicate (DHMS): the hydrous D phase [e.g., *Frost*, 2006; *Kawamoto*, 2006]. *Iwamori* [2004] and *Ohtani et al.* [2004] have shown that, along a cold slab geotherm, the hydrous D phase can replace ~50% of subducted peridotites, making it volumetrically abundant enough to potentially produce significant anisotropy. At TZ pressure–temperature conditions, a D phase single-crystal has a V_S anisotropy of ~17% [*Mainprice et al.*, 2007]. However, there are as yet no studies on deformation of the hydrous D phase and consequently no information about its LPO development.

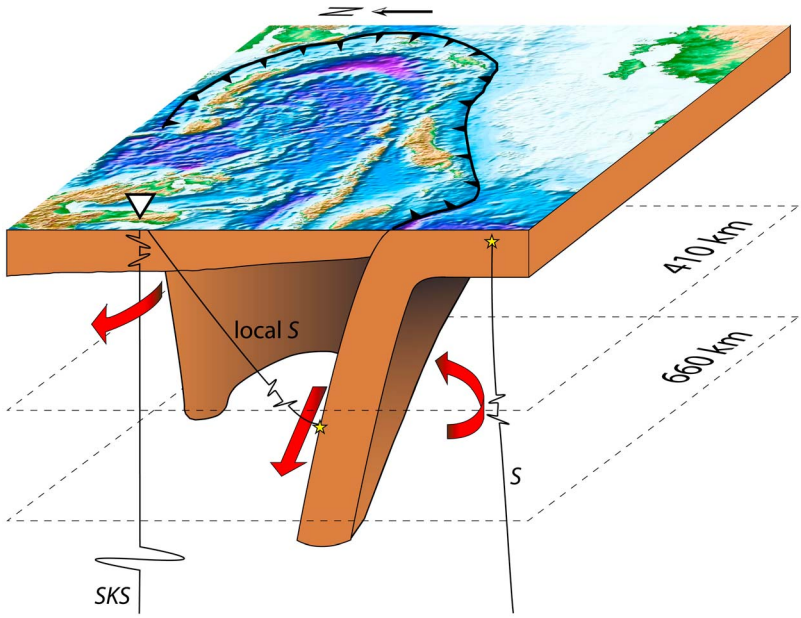

Figure 10. Cartoon illustrating mantle flow (red arrows) in the Banda subduction zone and raypaths of the different shear phases used in the splitting analysis. We detect different domains of seismic anisotropy related to mantle flow. The first is trench-parallel mantle flow paralleling the curvature of the Banda arc, both above and below the slab (as detected by *SKS* and source-side splitting, respectively). Secondly, we detect oblique supra-slab shear layers in the lower mantle wedge (detected by local *S* splitting).

Thus, we cannot confirm that the D phase in the subducted slab is the source of anisotropy; it is, however, a possible option.

[45] *Wookey et al.* [2002] detected similar deep anisotropy beneath the Tonga–Kermadec and New Hebrides subduction zones, with δt ranging from 0.6 s to 7.1 s. They proposed three different models to account for the measured splitting: pooling of slab material in the topmost lower mantle, strain-induced anisotropy around the leading edge of the slab, or an anisotropic boundary layer near the 660 km discontinuity. In an effort to explain these findings, *Nippress et al.* [2004] modeled subduction body force stresses in the uppermost lower mantle due to a viscosity increase at the 660 km discontinuity and predicted resultant shear wave splitting. The viscosity contrast impedes a slab as it descends [*Kusznir*, 2000], and this could potentially induce LPO, and thus seismic anisotropy, in the surrounding minerals, i.e., perovskite. *Nippress et al.* [2004] favor this scenario as an explanation for the deep seismic anisotropy observed by *Wookey et al.* [2002]. As the slab has reached a depth of ~700 km at the Sunda trench [*Gudmundsson and Sambridge*, 1998], we view this as a viable mechanism to account for the splitting that we measure here.

[46] Although we detect clear evidence for sub-520 km anisotropy, we cannot with certainty identify its cause, as this is beyond the scope of this study. A broader, global study of shear wave splitting in the mantle transition zone could potentially shed more light on this phenomenon.

6.2.3. Seismic Anisotropy in the Sumatran Backarc

[47] At the three stations in the Sumatran backarc (BTDF, TPN, TPI), we measure *SKS* splitting with time-lags between 0.68 s and 2.73 km. Although δt is quite varied, fast directions are consistently NE–SW trending, i.e., trench-perpendicular. Unfortunately, no other shear phases rendered splitting results at these stations for improved spatial constraints. Fast orientations are nearly perpendicular to those measured by *Hammond et al.* [2010], indicating that we are detecting a different region of anisotropy. There are no geological surface expressions of prominent tectonic features present which would suggest that the splitting is caused by fossil anisotropy of ancient lithospheric-scale faults [e.g., *Bastow et al.*, 2007, 2011]. Although we cannot rule out a small contribution from the crust, delay times caused by crack-induced crustal anisotropy are typically not more than ~0.2–0.3 s [*Gledhill*, 1991; *Gledhill and Gubbins*, 1995; *Morley et al.*, 2006]. We suggest that the bulk of the splitting is due to

olivine LPO in the upper mantle, either due to basal asthenospheric drag or corner flow in the mantle below the overriding Eurasian plate.

6.3. Region 3: Northern Sulawesi and the Molucca Sea

[48] With stacked averages of 1.25 s and 1.30 s, delay times measured at TOLI and LUWI, respectively, are similar in magnitude to those measured at MNI with δt of ~1.53 s [*Di Leo et al.*, 2012]. We ascribed this to trench-parallel sub-slab mantle flow due to double-sided subduction of the Molucca Sea plate. With the entire microplate sinking, the mantle is being squeezed outwards on both sides, parallel to the two trenches. Consequently, it seems likely that *SKS* phases recorded at LUWI are detecting this same mantle flow as it escapes the sinking plate. In the case of TOLI, fast directions are perpendicular to the strike of the Molucca Sea slab and oblique to the North Sulawesi trench. Placing depth constraints on this anisotropy is difficult, as no local *S* measurements were obtained at TOLI. The *SKS* rays are within the influence sphere of both subduction zones, so it is possible that both are contributing to the measured splitting. We relate the splitting measured at PCI to toroidal flow around the SE dipping Celebes Sea slab. Such toroidal flow around lateral slab edges has been observed both in analog [*Buttles and Olson*, 1998; *Schellart*, 2004] and numerical models [*Lowman et al.*, 2007]. Delay times are smaller than those recorded at TOLI, LUWI, and MNI with a stacked average of ~0.98 s. Unlike the Molucca Sea slab, however, the Celebes Sea slab has only reached a depth of ~200–250 km, and subduction is impeded by collision with the Molucca Sea slab [*Walpersdorf et al.*, 1998; *Kopp et al.*, 1999]. Therefore, it is not surprising that the anisotropic fabrics due to this toroidal flow are less extensive and less pronounced.

[49] Local *S* splitting recorded at PCI and LUWI complements measurements taken at MNI, located on the volcanic arc of the Sangihe subduction zone [*Di Leo et al.*, 2012]. In our recent study, we were able to distinguish two different regions of anisotropy in the Sangihe subduction zone due to the excellent depth distribution of local earthquakes. Events originating below ~380 km detected shear-layers atop the subducting slab, resulting in trench-normal fast directions. Local *S* phases of events shallower than ~380 km were sensitive to trench-parallel aligned cracks, perhaps melt-filled, in the overriding plate, thereby giving trench-parallel fast orientations. We suggest that local *S* splitting measured at LUWI and PCI is caused by these same phenomena in the Sangihe subduction zone.

6.4. Region 4: Borneo

[50] Delay times measured at the four Borneo stations are quite variable, ranging from 0.55 to 1.35 s. However, fast directions are fairly consistently parallel to the island's coast line. It is probable that this is due to fossil anisotropy, i.e., anisotropic fabrics frozen into the lithosphere, stemming from extensive counter-clockwise rotation of Borneo in the past. Paleomagnetic data suggest this rotation to have amounted to ~40° in the Late Cretaceous and ~45–50° between 25 and 10 Ma ago in the Miocene [*Fuller et al.*, 1999]. Fossil anisotropy bears evidence of the last significant episode of deformation and can remain intact over a long time in the absence volcanism or subsequent deformation [e.g., *Silver and Chan*, 1991; *Helffrich*, 1995; *Bastow et al.*, 2007]. Given the lack of subduction, volcanism or other significant deformation in Kalimantan since the Miocene, it is likely that the *SKS* phases are detecting fossil anisotropic fabrics created during rotation of Borneo in the past.

6.5. The Relation Between Subduction and Mantle Flow

[51] Despite progress having been made in the past few decades in comprehending subduction zone dynamics, several aspects are still not fully understood. This includes the role of subducted lithosphere in mantle convection or the coupling between plates and the underlying mantle. This set of observations in a tectonically complex region with several active plate margins provides us with a unique opportunity of studying the behavior of the mantle in subduction settings. We infer several different flow features in the upper mantle beneath Indonesia: toroidal flow around the Celebes Sea slab, oblique corner flow in the Banda wedge, trench-parallel flow beneath the arcuate Banda slab, trench-perpendicular flow in the Sumatran backarc, and potentially flow around the leading edge of the Indo-Australian slab. This implies that the discussion about whether mantle flow in subduction zones is either trench-perpendicular or -parallel, which has arisen from studies of seismic anisotropy, is perhaps oversimplified and that flow at convergent plate boundaries is more complex than previously believed. In most regions of oceanic lithosphere, observations of seismic anisotropy suggest mantle flow direction to be well correlated with the surface motion of oceanic plates [e.g., *Becker et al.*, 2003; *Conrad et al.*, 2007; *Becker*, 2008; *Kreemer*, 2009]. However, that may not

be true in regions of density driven mantle flow, such as hot spots or subduction zones [e.g., *Gaboret et al.*, 2003; *Hammond et al.*, 2005]. In the subduction zones of Indonesia, fast directions are neither uniformly perpendicular nor parallel to apparent plate motion. This has been observed in several other subduction zones as well, e.g., Kamchatka [*Peyton et al.*, 2001], South America [*Russo and Silver*, 1994], and the Marianas [*Pozgay et al.*, 2007]. Numerical studies of three-dimensional mantle convection in subduction systems have suggested as much [e.g., *Lowman et al.*, 2007; *Jadamec and Billen*, 2010, 2012]. They show that various factors - including slab geometry, morphology, and density; mantle viscosity; temperature gradients along the slab; plate configuration - can all lead to complex mantle flow patterns, including oblique or toroidal flow alongside trench-parallel and -perpendicular flow. *Jadamec and Billen* [2010, 2012] have argued that when assuming a composite viscosity of the mantle (i.e., Newtonian and non-Newtonian viscosity) and a power law rheology (which allows for deformation by dislocation creep), a partial decoupling between mantle and plates is possible. This is due to the fact that near subducting slabs, dislocation creep deformation rates are higher for a given stress (due to the power law relationship between strain rate and stress), which reduces the effective viscosity [e.g., *Karato et al.*, 2008]. A consequence of this is that at subduction zones, mantle flow velocities can be up to around eight times faster than surface plate motions, and mantle flow directions do not necessarily parallel plate trajectory [e.g., *Jadamec and Billen*, 2010, 2012].

[52] The architecture of the tectonic setting in Indonesia is largely prescribed by the geometry of pre-existing plate boundaries; the region, especially eastern Indonesia, is an amalgamation of various terranes and microplates. As they converged and coalesced, subduction was an inevitable consequence. This implies that the tectonic setting is a precondition for the resulting mantle flow. However, although the mantle is partially decoupled from the slabs, its movement is not simply a passive response to plate movement. The degree of decoupling between plates and mantle is still poorly constrained. Observations of mantle flow directions as inferred from seismic anisotropy can therefore provide predictions that can be modeled to explore the parameters controlling slab–mantle coupling.

7. Conclusions

[53] In this study, we present new shear wave splitting results for previously unstudied (with respect to seismic anisotropy) areas of Indonesia: the Sumatran backarc, Borneo (Kalimantan), southern Sulawesi, and the Banda Arc. We put these results into the broader context of the complex tectonic setting of Indonesia and previous studies by *Hammond et al.* [2010] and *Di Leo et al.* [2012]. Like the latter study, we use three different shear phases (local upgoing *S*, *SKS*, and downgoing *S* for source-side splitting) to obtain an improved spatial resolution of anisotropic fabrics. We demonstrate how this method can complement other techniques (e.g., studies of palaeomagnetics or GPS measurements) in unraveling the tectonic history of a region. For example, *SKS* measurements of Borneo show coast-parallel fast directions. This fossil anisotropy, frozen into the lithosphere below Borneo, reflects the island's history of counter-clockwise block rotation as first detected by paleomagnetism [e.g., *Fuller et al.*, 1999]. Moreover, seismic anisotropy may identify tectonic boundaries that cannot be detected when, for example, examining seismicity-derived slab surface models [*Gudmundsson and Sambridge*, 1998; *Syracuse and Abers*, 2006; *Hayes et al.*, 2012]. *Hammond et al.* [2010] have shown this to be the case for the Sunda Strait separating Sumatra from Java. Similarly, the highly varied fast directions recorded at station BMI southwest of Sulawesi reflect the boundary between the Sunda and the Banda Arc and thus the transition from subduction of oceanic to continental lithosphere. Furthermore, using upgoing and downgoing *S* phases, we are able to detect three different domains of anisotropy in the Banda subduction zone: trench-perpendicular to sub-perpendicular shear-layers atop the slab, as detected by local *S* phases, as well as deep-slab anisotropy and trench-parallel sub-slab anisotropy paralleling the curvature of the Banda arc, as detected by source-side splitting. In northern Sulawesi, local *S* and *SKS* splitting results complement findings by *Di Leo et al.* [2012] for the Sangihe subduction zone. We attribute the trench-parallel anisotropy measured at LUWI to sub-slab mantle flow associated with double-sided subduction of the Molucca Sea microplate. We ascribe E–W trending fast directions measured at PCI to toroidal flow around the edge of the Celebes Sea slab at the North Sulawesi subduction zone. Finally, we measure trench-perpendicular fast directions in the Sumatran backarc that we ascribe to mantle flow below the overriding Eurasian plate.

[54] By using careful, multiphase studies of seismic anisotropy in conjunction with other geophysical and geological evidence, we can pick apart the signal associated with even a very complex tectonic

history. We observe mantle flow which is different than - but apparently related to - these complex tectonics. This has implications for the nature of the coupling between subducting plates and the underlying mantle.

Acknowledgments

[55] The research leading to these results has received funding from Crystal2Plate, an FP7-funded Marie Curie Action under grant agreement number PITN-GA-2008-215353, and from the European Research Council under the European Union's Seventh Framework Program (FP7/2007-2013)/ERC Grant agreement 240473 'CoMITAC'. Data used in this study was provided by GEOFON and the Japan Indonesian Seismic Network (JISNET), courtesy of the Earthquake Research Institute, University of Tokyo. Several figures were created using the GMT software [*Wessel and Smith*, 1991]. We thank T. Becker, B. Foley and an anonymous reviewer for their comments.

References

Abbott, M. J., and F. H. Chamalaun (1981), Geochronology of some Banda Arc volcanics, in *The Geology and Tectonics of Eastern Indonesia*, edited by A. J. Barber and S. Wiryosujono, *Geol. Res. Dev. Cent. Spec. Publ.*, *2*, 253–268.

Artemieva, I. M., and W. D. Mooney (2001), Thermal thickness and evolution of Precambrian lithosphere: A global study, *J. Geophys. Res.*, *106*(B8), 16,387–16,414.

Aurelio, M. (1992), Tectonique du segment central de la Faille Philippine: Étude structurale, cinématique et évolution géodynamique, thèse de doctorat, 345 pp., Univ. Pierre et Marie Curie, Paris.

Babuška, V., and M. Cara (1991), *Seismic Anisotropy in the Earth*, Kluwer Acad., Norwell, Mass.

Bader, A. G., and M. Pubellier (2000), Forearc deformation and tectonic significance of the ultramafic Molucca central ridge, Talaud islands (Indonesia), *Isl. Arc*, *9*, 653–663.

Barber, A. J., M. J. Crow, and J. S. Milsom (Eds.) (2005), *Sumatra: Geology, Resources and Tectonic Evolution*, *Geol. Soc. London Mem.*, *31*.

Barruol, G., and R. Hoffmann (1999), Upper mantle anisotropy beneath the Geoscope stations, *J. Geophys. Res.*, *104*(B5), 10,757–10,773.

Bastow, I. D., T. J. Owens, G. Helffrich, and J. H. Knapp (2007), Spatial and temporal constraints on sources of seismic anisotropy: Evidence from the Scottish highlands, *Geophys. Res. Lett.*, *34*, L05305, doi:10.1029/2006GL028911.

Bastow, I. D., S. Pilidou, J.-M. Kendall, and G. W. Stuart (2010), Melt-induced seismic anisotropy and magma assisted rifting in Ethiopia: Evidence from surface waves, *Geochem. Geophys. Geosyst.*, *11*, Q0AB05, doi:10.1029/2010GC003036.

Bastow, I. D., D. Thompson, J. Wookey, J.-M. Kendall, G. Helffrich, D. Snyder, D. Eaton, and F. A. Darbyshire (2011), Precambrian plate tectonics: Seismic evidence from northern Hudson Bay, Canada, *Geology*, *39*, 91–94, doi:10.1130/G31396.1.

Becker, T. W. (2008), Azimuthal seismic anisotropy constrains net rotation of the lithosphere, *Geophys. Res. Lett.*, *35*, L05303, doi:10.1029/2007GL032928.

Becker, T. W., J. B. Kellogg, G. Ekstrom, and R. J. O'Connell (2003), Comparison of azimuthal seismic anisotropy from surface waves and finite strain from global mantle-circulation models, *Geophys. J. Int.*, *155*, 696–714.

Ben-Avraham, Z., and K. O. Emery (1973), Structural framework of Sunda Shelf, *AAPG Bull.*, *57*, 2323–2366.

Bercovici, D., and S. Karato (2003), Whole-mantle convection and the transition-zone water filter, *Nature*, *425*, 39–44.

Buttles, J., and P. Olson (1998), A laboratory model of subduction zone anisotropy, *Earth Planet. Sci. Lett.*, *164*, 245–262.

Cardwell, R. K., and B. L. Isacks (1978), Geometry of the subducted lithosphere beneath the Banda Sea in eastern Indonesia from seismicity and fault plane solutions, *J. Geophys. Res.*, *83*, 2825–2838.

Carrez, P., P. Cordier, D. Mainprice, and A. Tommasi (2006), Slip systems and plastic shear anisotropy in Mg_2SiO_4 ringwoodite: Insights from numerical modelling, *Eur. J. Mineral.*, *18*, 149–160.

Charlton, T. R. (2000), Tertiary evolution of the Eastern Indonesia Collision Complex, *J. Asian Earth Sci.*, *18*, 603–631.

Cloke, I. R., J. Milsom, and D. J. B. Blundell (1999), Implications of gravity data from east Kalimantan and the Makassar Straits: A solution to the origin of the Makassar Straits?, *J. Asian Earth Sci.*, *17*, 61–78.

Conrad, C. P., M. D. Behn, and P. G. Silver (2007), Global mantle flow and the development of seismic anisotropy: Differences between the oceanic and continental upper mantle, *J. Geophys. Res.*, *112*, B07317, doi:10.1029/2006JB004608.

Crampin, S., and D. C. Booth (1985), Shear-wave polarizations near the North Anatolian Fault, II, Interpretation in terms of crack-induced anisotropy, *Geophys. J. R. Astron. Soc.*, *92*, 75–92.

Crotwell, H. P., T. J. Owens, and J. Ritsema (1999), The TauP Toolkit: Flexible seismic travel-time and ray-path utilities, *Seismol. Res. Lett.*, *70*, 154–160.

Demouchy, S., D. Mainprice, A. Tommasi, H. Couvy, F. Barou, D. J. Frost, and P. Cordier (2011), Forsterite to wadsleyite phase transformation under shear stress and consequences for the Earth's mantle transition zone, *Phys. Earth Planet. Int.*, *184*, 91–104.

Di Leo, J., J. Wookey, J. O. S. Hammond, J.-M. Kendall, S. Kaneshima, H. Inoue, T. Yamashina, and P. Harjadi (2012), Deformation and mantle flow beneath the Sangihe subduction zone from seismic anisotropy, *Phys. Earth Planet. Int.*, *194–195*, 38–54, doi:10.1016/j.pepi.2012.01.008.

Djajadihardja, Y. S., A. Taira, H. Tokuyama, K. Aoike, C. Reichert, M. Block, H. U. Schluter, and S. Neben (2004), Evolution of an accretionary complex along the north arm of the island of Sulawesi, Indonesia, *Isl. Arc*, *13*, 1–17.

Engdahl, E., R. van der Hilst, and R. Buland (1998), Global teleseismic earthquake relocation with improved travel times and procedures for depth determination, *Bull. Seismol. Soc. Am.*, *88*(3), 722–743.

Frost, D. J. (2006), The stability of hydrous mantle phases, *Rev. Mineral. Geochem.*, *62*, 243–271.

Fuller, M., J. R. Ali, S. J. Moss, G. M. Frost, B. Richter, and A. Mahfi (1999), Paleomagnetism of Borneo, *J. Asian Earth Sci.*, *17*, 3–24.

Gaboret, C., A. M. Forte, and J.-P. Montagner (2003), The unique dynamics of the Pacific Hemisphere mantle and its signature on seismic anisotropy, *Earth Planet. Sci. Lett.*, *208*, 219–233.

Gledhill, K. R. (1991), Evidence for shallow and pervasive anisotropy in the Wellington region, New Zealand, *J. Geophys. Res.*, *96*, 21,503–21,516.

Gledhill, K., and D. Gubbins (1995), SKS splitting and the seismic anisotropy of the mantle beneath the Hikurangi subduction zone, New Zealand *Phys. Earth Planet. Int.*, *95*, 227–236.

Gorbatov, A., and B. L. N. Kennett (2003), Joint bulk–sound and shear tomography for Western Pacific subduction zones, *Earth Planet. Sci. Lett.*, *210*, 527–543.

Gordon, R. G. (1998), The plate tectonic approximation: Plate nonrigidity, diffuse plate boundaries, and global plate reconstructions, *Annu. Rev. Earth Planet. Sci.*, *26*, 615–642.

Greve, S. M., M. K. Savage, and S. D. Hofmann (2008), Strong variations in seismic anisotropy across the Hikurangi subduction zone, North Island, New Zealand. *Tectonophysics*, *462*, 7–21.

Gripp, A. E., and R. G. Gordon (1990), Current plate motions relative to the hotspots incorporating the NUVEL–1 global plate motion model, *Geophys. Res. Lett.*, *17*, 1109–1112.

Gudmundsson, Ó., and M. Sambridge (1998), A regionalized upper mantle (RUM) seismic model, *J. Geophys. Res.*, *103*(B4), 7121–7136.

Hall, R. (1997), Cenozoic plate tectonic reconstructions of SE Asia, *Geol. Soc. Spec. Publ.*, *126*, 11–23.

Hall, R. (2002), Cenozoic geological and plate tectonic evolution of SE Asia and the SW Pacific: Computer-based reconstructions, model and animations, *J. Asian Earth Sci.*, *20*, 353–431.

Hall, R. (2009), The Eurasian SE Asian margin as a modern example of an accretionary orogen, *Geol. Soc. Spec. Publ.*, *318*, 351–372.

Hall, R. (2012), Late Jurassic–Cenozoic reconstructions of the Indonesian region and the Indian Ocean, *Tectonophysics*, *570–571*, 1–41.

Hall, R., and C. K. Morley (2004), Sundaland basins, in *Continent–Ocean Interactions Within the East Asian Marginal Seas*, *Geophys. Monogr. Ser.*, vol. 149, edited by P. Clift et al., pp. 55–85, AGU, Washington, D. C., doi:10.1029/149GM04.

Hall, R., and G. J. Nichols (1990), Terrane amalgamation in the Philippine Sea margin, *Tectonophysics*, *181*, 207–222.

Hall, R., M. W. A. van Hattum, and W. Spakman (2008), Impact of India–Asia collision on SE Asia: The record in Borneo, *Tectonophysics*, *451*, 366–389.

Hamilton, W. (1979), Tectonics of the Indonesian region, *U.S. Geol. Surv. Prof. Pap.*, *1078*, 345 pp.

Hamilton, W. B. (1988), Plate tectonics and island arcs, *Geol. Soc. Am. Bull.*, *100*, 1503–1527.

Hammond, J. O. S., J. Wookey, S. Kaneshima, H. Inoue, T. Yamashina, and P. Harjadi (2010), Systematic variation in anisotropy beneath the mantle wedge in the Java-Sumatra subduction system from shear-wave splitting, *Phys. Earth Planet. Int.*, *178*, 189–201.

Hammond, W. C., J.-M. Kendall, G. Rümpker, J. Wookey, N. Teanby, P. Joseph, T. Ryberg, and G. Stuart (2005), Upper mantle anisotropy beneath the Seychelles microcontinent, *J. Geophys. Res.*, *110*, B11401, doi:10.1029/2005JB003757.

Hayes, G. P., D. J. Wald, and R. L. Johnson (2012), Slab1.0: A three-dimensional model of global subduction zone geometries, *J. Geophys. Res.*, *117*, B01302, doi:10.1029/2011JB008524.

Helffrich, G. (1995), Lithospheric deformation inferred from teleseismic shear wave splitting observations in the United Kingdom, *J. Geophys. Res.*, *100*(B9), 18,195–18,204.

Holtzman, B. K., and J.-M. Kendall (2010), Organized melt, seismic anisotropy, and plate boundary lubrication, *Geochem. Geophys. Geosyst.*, *11*, Q0AB06, doi:10.1029/2010GC003296.

Hutchinson, C. S. (2006), The Rajang accretionary prism and Lupar Line problem of Borneo, in *Tectonic Evolution of SE Asia*, edited by R. Hall and D. J. Blundell, *Geol. Soc. Spec. Publ.*, *106*, 247–261.

Iwamori, H. (2004), Phase relations of peridotites under H_2O-saturated conditions and ability of subducting plates for transportation of H_2O, *Earth Planet. Sci. Lett.*, *227*, 57–71.

Jadamec, M. A., and M. I. Billen (2010), Reconciling surface plate motions with rapid three-dimensional mantle flow around a slab edge, *Nature*, *465*, 338–342, doi:10.1038/nature09053.

Jadamec, M. A., and M. I. Billen (2012), The role of rheology and slab shape on rapid mantle flow: Three-dimensional numerical models of the Alaska slab edge, *J. Geophys. Res.*, *117*, B02304, doi:10.1029/2011JB008563.

Jaffe, L. A., D. R. Hilton, T. P. Fischer, and U. Hartono (2004), Tracing magma sources in an arc-arc collision zone: Helium and carbon isotope and relative abundance systematics of the Sangihe Arc, Indonesia, *Geochem. Geophys. Geosyst.*, *5*, Q04J10, doi:10.1029/2003GC000660.

Kaneshima, S., and M. Ando (1989), An analysis of split shear waves observed above crustal and uppermost mantle earthquakes beneath Shikoku, Japan: Implications in effective depth extent of seismic anisotropy, *J. Geophys. Res.*, *94*(B10), 14,077–14,092.

Kaneshima, S., M. Ando, and S. Kimura (1988), Evidence from shear-wave splitting for the restriction of seismic anisotropy to the upper crust, *Nature*, *335*, 627–629.

Karato, S., H. Jung, I. Katayama, and P. Skemer (2008), Geodynamic significance of seismic anisotropy of the upper mantle: New insights from laboratory studies, *Annu. Rev. Earth Planet. Sci.*, *36*, 59–95, doi:10.1146/annurev.earth.36.031207.124120.

Kawamoto, T. (2006), Hydrous phases and water transport in the subducting slab, *Rev. Mineral. Geochem.*, *62*, 273–289.

Kendall, J.-M., and C. J. Thomson (1993), Seismic modelling of subduction zones with inhomogeneity and anisotropy – I. Teleseismic P-wavefront tracking, *Geophys. J. Int.*, *112*, 39–66.

Kendall, J.-M., G. W. Stuart, C. J. Ebinger, I. D. Bastow, and D. Keir (2005), Magma assisted rifting in Ethiopia, *Nature*, *433*, 146–148.

Kennett, B., and E. Engdahl (1991), Traveltimes from global earthquake location and phase identification, *Geophys. J. Int.*, *105*(2), 429–465.

Kopp, C., E. R. Flueh, and S. Neben (1999), Rupture and accretion of the Celebes Sea crust related to the North-Sulawesi subduction: Combined interpretation of reflection and refraction seismic measurements, *Geodynamics*, *27*, 309–325.

Kreemer, C. (2009), Absolute plate motions constrained by shear wave splitting orientations with implications for hot spot motions and mantle flow, *J. Geophys. Res.*, *114*, B10405, doi:10.1029/2009JB006416.

Kustowski, B., G. Ekström, and A. Dziewoński (2008), Anisotropic shear-wave velocity structure of the Earth's mantle: A global model, *J. Geophys. Res.*, *113*, B06306, doi:10.1029/2007JB005169.

Kusznir, N. J. (2000), Subduction body force stresses and viscosity structure at the 410 km and 660 km phase transition, *Eos Trans. AGU*, *81*(48), 1081.

Lee, T.-Y., and A. L. Lawrence (1995), Cenozoic plate reconstruction of Southeast Asia, *Tectonophysics*, *251*, 85–138.

Long, M. D., and T. W. Becker (2010), Mantle dynamics and seismic anisotropy, *Earth Planet. Sci. Lett.*, *279*, 341–354.

Long, M. D., and P. G. Silver (2009), Mantle flow in subduction systems: The subslab flow field and implications for mantle dynamics, *J. Geophys. Res.*, *114*, B10312, doi:10.1029/2008JB006200.

Lowman, J. P., L. T. Piñero-Feliciangeli, J.-M. Kendall, and M. Hosein Shahnas (2007), Influence of convergent plate boundaries on upper mantle flow and implications for seismic anisotropy, *Geochem. Geophys. Geosyst.*, *8*, Q08007, doi:10.1029/2007GC001627.

Macpherson, C. G., and R. Hall (2002), The timing and location of major ore deposits in an evolving orogen, *Geol. Soc. Spec. Publ.*, *204*, 49–67.

Macpherson, C. G., E. J. Forrde, R. Hall, and M. F. Thirlwall (2003), Geochemical evolution of magmatism in an arc-arc collision: The Halmahera and Sangihe arcs, eastern Indonesia, *Geol. Soc. Spec. Publ.*, *219*, 207–220.

Mainprice, D. (2007), Seismic anisotropy of the deep Earth from a mineral and rock physics perspective, *Treatise Geophys.*, *2*, 437–492.

Mainprice, D., M. Humbert, and F. Wagner (1990), Phase-transformations and inherited lattice preferred orientations–Implication for seismic properties, *Tectonophysics*, *180*(2–4), 213–228.

Mainprice, D., Y. Le Page, J. Rodgers, and P. Jouanna (2007), Predicted elastic properties of the hydrous D phase at mantle pressures: Implications for the anisotropy of subducted slabs near 670-km discontinuity and in the lower mantle, *Earth Planet. Sci. Lett.*, *259*, 283–296.

McCaffrey, R. (1989), Seismological constraints and speculations on Banda arc tectonics, *Neth. J. Sea Res.*, *24*, 141–152.

McKenzie, D. (1979), Finite deformation during fluid flow, *Geophys. J. R. Astron. Soc.*, *58*, 689–715.

Meade, C., P. G. Silver, and S. Kaneshima (1995), Laboratory and seismological observations of lower mantle isotropy, *Geophys. Res. Lett.*, *22*, 1293–1296.

Montagner, J.-P., and B. Kennett (1996), How to reconcile body-wave and normal-mode reference Earth models, *Geophys. J. Int.*, *125*, 229–248.

Morley, A. M., G. W. Stuart, J.-M. Kendall, and M. Reyners (2006), Mantle wedge anisotropy in the Hikurangi subduction zone, central North Island, New Zealand, *Geophys. Res. Lett.*, *33*, L05301, doi:10.1029/2005GL024569.

Nippress, S. E. J., N. J. Kusznir, and J.-M. Kendall (2004), Modeling of lower mantle seismic anisotropy beneath subduction zones, *Geophys. Res. Lett.*, *31*, L19612, doi:10.1029/2004GL020701.

Nowacki, A., J.-M. Kendall, and J. Wookey (2012), Mantle anisotropy beneath the Earth's mid-ocean ridges, *Earth Planet. Sci. Lett.*, *317–318*, 56–67.

Ohtaki, T., K. Kanjo, S. Kaneshima, T. Nishimura, Y. Ishihara, Y. Yoshida, S. Harada, and S. Kamiya (2000), Sunarjo, broadband seismic network in Indonesia-JISNET, *Bull. Geol. Surv. Jpn.*, *51*, 189–203.

Ohtani, E., K. Litasov, T. Hosoya, T. Kubo, and T. Kondo (2004), Water transport into the deep mantle and formation of a hydrous transition zone, *Phys. Earth Planet. Int.*, *143*, 255–269.

Panning, M., and B. Romanowicz (2006), A three-dimensional radially anisotropic model of shear velocity in the whole mantle, *Geophys. J. Int.*, *167*, 361–379.

Peyton, V., V. Levin, J. Park, M. Brandon, J. Lees, E. Gordeev, and A. Ozerov (2001), Mantle flow at a slab edge: Seismic anisotropy in the Kamchatka region, *Geophys. Res. Lett.*, *28*, 379–382.

Piñero-Feliciangeli, L. T., and J.-M. Kendall (2008), Sub-slab mantle flow parallel to the Caribbean plate boundaries: Inferences from SKS splitting, *Tectonophysics*, *462*, 22–34.

Pozgay, S. H., D. A. Wiens, J. A. Conder, H. Shiobara, and H. Sugioka (2007), Complex mantle flow in the Mariana subduction system: Evidence from shear wave splitting, *Geophys. J. Int.*, *170*(1), 371–386.

Ribe, N. M. (1989), Seismic anisotropy and mantle flow, *J. Geophys. Res.*, *94*(B4), 4213–4223.

Ritsema, J., and H. van Heijst (2000), New seismic model of the upper mantle beneath Africa, *Geology*, *28*(1), 63–66.

Russo, R. M., and P. G. Silver (1994), Trench-parallel flow beneath the Nazca Plate from seismic anisotropy, *Science*, *263*, 1105–1111.

Sajona, F. G., H. Bellon, R. Maurg, M. Pubellier, R. D. Quebral, J. Cotton, F. E. Bayon, E. Pagado, and P. Pamatian (1997), Tertiary and Quaternary magmatism in Mindanao and Leyte (Philippines): Geochronology, geochemistry and tectonic setting, *J. Asian Earth Sci.*, *15*(2–3), 121–153.

Schellart, W. P. (2004), Kinematics of subduction and subduction-induced flow in the upper mantle, *J. Geophys. Res.*, *109*, B07401, doi:10.1029/2004JB002970.

Sdrolias, M., and R. D. Müller (2006), Controls on back-arc basin formation, *Geochem. Geophys. Geosyst.*, *7*, Q04016, doi:10.1029/2005GC001090.

Silver, E. A., and R. B. Smith (1983), Comparison of terrane accretion in modern Southeast Asia and the Mesozoic North American Cordillera, *Geology*, *11*, 198–202.

Silver, P., and G. Chan (1991), Shear wave splitting and subcontinental mantle deformation, *J. Geophys. Res.*, *96*, 16,429–16,454.

Silver, P. G., and M. K. Savage (1994), The interpretation of shear wave splitting parameters in the presence of two anisotropic layers, *Geophys. J. Int.*, *119*, 949–963.

Smyth, H. R., R. Hall, and G. J. Nichols (2008), Early Cenozoic volcanic arc history of East Java, Indonesia: The stratigraphic record of eruptions on a continental margin in a tropical setting, in *Formation and Applications of the Sedimentary Record in Arc Collision Zones*, edited by A. E. Draut, P. D. Clift, and D. W. Scholl, *Geol. Soc. Am. Spec. Publ.*, *436*, 199–222.

Snyder, D. B., and A. J. Barber (1997), Australia-Banda Arc collision as an analogue for early stages in Iapetus closure, *J. Geol. Soc. London*, *154*, 589–592.

Spakman, W., and R. Hall (2010), Surface deformation and slab–mantle interaction during Banda Arc subduction rollback, *Nat. Geosci.*, *3*, 562–566.

Syracuse, E. M., and G. A. Abers (2006), Global compilation of variations in slab depth beneath arc volcanoes and implications, *Geochem. Geophys. Geosyst.*, *7*, Q05017, doi:10.1029/2005GC001045.

Teanby, N. A., J.-M. Kendall, and M. van der Baan (2004), Automation of shear-wave splitting measurements using cluster analysis, *Bull. Seismol. Soc. Am.*, *94*(2), 453–463.

Tjia, H. D. (1996), Sea-level changes in the tectonically stable Malay–Thai peninsula, *Quat. Int.*, *31*, 95–101.

Tommasi, A., and D. Mainprice (2008), Comment on the article "Probability of radial anisotropy in the deep mantle" by Visser et al. (2008) EPSL 270:241–250, *Earth Planet. Sci. Lett.*, *276*, 223–225.

Tommasi, A., D. Mainprice, P. Cordier, and C. Thoraval (2004), Strain-induced seismic anisotropy of wadsleyite polycrystals and flow patterns in the mantle transition zone, *J. Geophys. Res.*, *109*, B12405, doi:10.1029/2004JB003158.

Walpersdorf, A., C. Rangin, and C. Vigny (1998), GPS compared to long-term geologic motion of the north arm of Sulawesi, *Earth Planet. Sci. Lett.*, *159*, 47–55.

Wessel, P., and W. H. F. Smith (1991), Free software helps map and display data, *Eos Trans. AGU*, *72*(41), 441.

Whittaker, J. M., R. D. Müller, M. Sdrolias, and C. Heine (2007), Sunda–Java trench kinematics, slab window formation and

overriding plate deformation since the Cretaceous, *Earth Planet. Sci. Lett.*, *255*, 445–457.

Widiyantoro, S., and R. V. van der Hilst (1997), Mantle structure beneath Indonesia inferred from high-resolution tomographic imaging, *Geophys. J. Int.*, *130*, 167–182.

Winchester, J., and H. P. Crotwell (1999), Electronic seismologist: WebWEED and TauP: Java and seismology, *Seismol. Res. Lett.*, *70*(1), 81–84, doi:10.1785/gssrl.70.1.81.

Wolfe, C. J., and P. G. Silver (1998), Seismic anisotropy of oceanic upper mantle: Shear wave splitting methodologies and observations, *J. Geophys. Res.*, *103*(B1), 749–771.

Wolfe, C. J., and F. L. Vernon (1998), Shear-wave splitting at central Tien Shan: Evidence for rapid variation of anisotropic patterns, *Geophys. Res. Lett.*, *25*(8), 1217–1220.

Wookey, J., J.-M. Kendall, and G. Barruol (2002), Mid-mantle deformation inferred from seismic anisotropy, *Nature*, *415*, 777–780.

Wookey, J., J.-M. Kendall, and G. Rümpker (2005), Lowermost mantle anisotropy beneath the north Pacific from differential *S*–*ScS* splitting, *Geophys. J. Int.*, *161*, 829–838.

Wüstefeld, A., O. Al-Harrasi, J. P. Verdon, J. Wookey, and J.-M. Kendall (2010), A strategy for automated analysis of passive microseismic data to image seismic anisotropy and fracture characteristics, *Geophys. Prospect.*, *58*, 755–773.